



1 A GLUE-based assessment of WaTEM/SEDEM for simulating soil 2 erosion, transport, and deposition in soil conservation optimised 3 agricultural watersheds

4 Kay D. Seufferheld¹, Pedro V. G. Batista¹, Hadi Shokati², Thomas Scholten², Peter Fiener¹

5 ¹Institute of Geography, Water and Soil Resources Research, University of Augsburg, Augsburg, 86159, Germany.

6 ²Department of Geosciences, Soil Science and Geomorphology, University of Tübingen, 72074, Tübingen,
 7 Germany.

8 *Correspondence to:* Peter Fiener (peter.fiener@geo.uni-augsburg.de, Alter Postweg 118, 56159 Augsburg,
 9 Germany)

10 **Abstract.** Soil erosion models are essential tools for soil conservation planning. Although these models are
 11 generally well-tested against plot and field data for in-field soil management, challenges arise when scaling up to
 12 the landscape level, where sediment trapping along landscape features becomes increasingly critical. At this scale,
 13 a separate analysis of model performance in representing erosion, sediment transport, and deposition processes
 14 is both challenging and often lacking. In this study, we assessed the capacity of the spatially distributed erosion
 15 and sediment transport model WaTEM/SEDEM to simulate sediment yields in six micro-scale watersheds ranging
 16 from 0.8 to 7.8 ha, monitored over eight years from 1994 to 2001. The watersheds were comprised of two groups:
 17 four field-dominated watersheds characterised by arable land with minimal landscape structures, and two
 18 structure-dominated watersheds featuring a combination of arable land and linear landscape structures (mainly
 19 grassed waterways along thalwegs) that minimise sediment connectivity. This setup enabled a separate analysis
 20 of model performance for both watershed groups. A Generalised Likelihood Uncertainty Estimation (GLUE)
 21 framework was employed to account for measurement and model uncertainties across multiple spatiotemporal
 22 scales. Our results show that while WaTEM/SEDEM generally captured the magnitude of the very low measured
 23 sediment yields in the monitored watersheds, the model did not meet our pre-defined limits of acceptability
 24 when operating on annual timesteps. However, the WaTEM/SEDEM's performance improved substantially when
 25 model realisations were aggregated across the eight-year monitoring period and over the two watershed groups,
 26 with mean absolute errors of 0.11 t ha⁻¹ yr⁻¹ for field-dominated and 0.18 t ha⁻¹ yr⁻¹ for structure-dominated
 27 watersheds. Our findings demonstrate that the model can represent the influence of soil conservation measures
 28 on reducing soil erosion and sediment delivery but performs better for long-term conservation planning at larger
 29 scales than for precise annual predictions in individual micro-scale watersheds with specific conservation
 30 practices.

31



32 1. Introduction

33 Soil erosion by water is a major threat to global soil health and associated ecosystem functions and services,
34 endangering agricultural sustainability and food security (Rickson et al., 2015; Montanarella et al., 2016; Quinton
35 and Fiener, 2024). Although the problem of accelerated soil erosion has been known for a long time and a wide
36 variety of soil conservation practices have been tested and implemented locally for many decades, adoption
37 remains limited due to economic constraints, lack of technical knowledge, and insufficient policy support
38 (Quinton and Fiener, 2024; Aghabeygi et al., 2024). This is particularly problematic in regions where the
39 intensification of agriculture, exemplified by the historical increase in the size and weight of agricultural
40 machinery that has led to increased soil compaction levels (Brus and Van Den Akker, 2018; Keller et al., 2019),
41 and the increase in frequency and intensity of extreme precipitation events due to climate change (Auerswald
42 and Fiener, 2024; Hosseinzadehtalaei et al., 2020; Myhre et al., 2019) is likely exacerbating the erosion risk.

43 Effective soil conservation relies on two complementary strategies: (i) In-field control measures that increase soil
44 surface cover by vegetation and hence prevent soil detachment by raindrop impact and sheet flow. Such
45 measures include optimised crop rotations, using cover crops, and soil residue management (Andersson and
46 D'souza, 2014). (ii) Off-site sediment transport control structures along the runoff pathway that increase
47 infiltration and foster sediment trapping and minimise sediment connectivity. Typical structures are vegetative
48 filter strips (Gumiere et al., 2011), grassed waterways (Fiener and Auerswald, 2003), retention ponds (Fiener et
49 al., 2005), or a generally optimised layout of fields along slopes (Van Oost et al., 2000).

50 Soil erosion models are potentially valuable tools for identifying high erosion risk areas and evaluating
51 intervention needs, enabling stakeholders to effectively implement soil conservation strategies. Diverse models
52 have been developed and applied for this purpose, ranging from empirical and conceptual to process-oriented
53 model types (e.g. Eekhout et al., 2018; Smith et al., 2018; Nearing, 2013; Dymond et al., 2010; Hessel and Tenge,
54 2008). The most widely used model for soil conservation planning is the Universal Soil Loss Equation (USLE)
55 (Wischmeier and Smith, 1978) and its revisions and regional adaptations, like the revised USLE (RUSLE) (Renard,
56 1997) and the German ABAG (Allgemeine Bodenabtragsgleichung, German for Universal Soil Loss Equation; Din-
57 Normenausschuss, 2022; Schwertmann et al., 1987).

58 While these USLE-type models have been adapted to calculate spatially distributed erosion rates, they are limited
59 to calculating potential soil loss without considering sediment transport processes and downslope deposition. To
60 overcome this limitation, the Water and Tillage Erosion Model and the Sediment Delivery Model
61 (WaTEM/SEDEM) (Van Oost et al., 2000; Van Rompaey et al., 2001; Verstraeten et al., 2002) was developed.
62 WaTEM/SEDEM combines the RUSLE (Renard, 1997) with spatially distributed sediment transport and deposition
63 modelling. The performance of the model has been tested using sediment trapping in reservoirs (e.g. Hlavčová
64 et al., 2018), sediment delivery in small rivers of mesoscale catchments (e.g. Batista et al., 2022; Rehm and Fiener,
65 2024), or long-term erosion and deposition patterns derived from radionuclides (e.g. Van Oost et al., 2000; Wilken
66 et al., 2020). However, to the best of our knowledge, the suitability of WaTEM/SEDEM for representing soil
67 erosion, transport, and deposition processes within soil conservation settings combined with measures to reduce
68 sediment connectivity, which can minimize sediment redistribution, has not been thoroughly tested.



69 Testing the ability of spatially distributed erosion models to simulate the combined effects of in-field soil
 70 conservation and landscape features trapping sediments is inherently challenging. Observational data for model
 71 calibration and validation are typically restricted to measurements of sediment yields at the outlet of a system
 72 (Batista et al., 2019), which typically consist of small erosion plots, meso-scale watersheds, or large-scale
 73 catchments. Such outlet-based measurements do not allow for testing a model's representation of internal
 74 erosion and deposition patterns, as they provide little information on the spatial distribution of sediment sources
 75 and sinks within the landscape. This exacerbates the equifinality problem (Beven, 2006), and models may achieve
 76 accurate outputs while incorrectly representing the spatial patterns of erosion and deposition processes within
 77 watersheds.

78 Micro-scale watersheds (1-10 ha) are ideal for evaluating soil conservation measures typically implemented from
 79 the field to the landscape level (Choudhury et al., 2022; Fiener and Auerswald, 2018). This is because soil erosion
 80 and sediment connectivity processes that are distinguishable at the micro-scale watershed are not represented
 81 in small plots or get diluted in large-catchment sediment yield observations. Moreover, important input data for
 82 erosion modelling, e.g. rainfall, soil management, and land cover, can be monitored and measured with higher
 83 detail at the micro-scale, compared to larger areas (Fiener et al., 2019a). Nevertheless, there is limited research
 84 on modelling the combined effects of in-field soil conservation and landscape structures on soil redistribution
 85 and sediment delivery at this scale.

86 Notwithstanding the spatial extent of (long-term) soil erosion monitoring, measurement uncertainties arise from
 87 instrumental precision and temporal instrument malfunctioning, data handling and processing. The uncertainties
 88 in observational data have important implications for erosion modelling, as models cannot be expected to be
 89 better than the observational data (Beven and Lane, 2022; Beven, 2019).

90 The Generalized Likelihood Uncertainty Estimation (GLUE) framework (Beven and Binley, 1992) allows for testing
 91 environmental models while accounting for the uncertainty in both models and the observational data. In light
 92 of inherent measurement uncertainties, GLUE acknowledges that it is not possible to identify a single parameter
 93 set as “correct”. Rather, all parameter combinations that produce results within the observational uncertainty
 94 cannot be rejected. Within the GLUE framework, limits of acceptability are defined to identify which model runs
 95 fall within the uncertainty bounds of the measurements (Beven and Lane, 2022). These behavioural models are
 96 retained, while non-behavioural models are rejected. This limits-of-acceptability GLUE approach thus provides a
 97 systematic methodology to evaluate model performance with uncertain testing data.

98 In this study we employ this limit-of-acceptability approach based on the GLUE framework, focusing on three
 99 main objectives: (i) testing WaTEM/SEDEM's capability to simulate sediment yields in micro-scale watersheds
 100 either characterised by in-field soil conservation or by in-field soil conservation plus linear landscape features
 101 designed to trap sediments, (ii) analysing the behaviour of model parameters that control erosion and sediment
 102 transport processes, and (iii) assessing the model's performance across different spatiotemporal resolutions
 103 through data aggregation. We accomplish these objectives using a comprehensive dataset from a long-term,
 104 farm-scale monitoring in Southern Germany, which provides continuous precipitation, surface runoff and



105 sediment flux data from six micro-scale watersheds under optimised soil conservation (Auerswald et al., 2001;
 106 Auerswald and Fiener, 2019).

107 2. Material and methods

108 2.1 Test site

109 The test site is part of an experimental farm located in Scheyern, southern Germany (48°29'45.1"N, 11°26'23.6"E;
 110 about 470 m above sea level). It is part of Bavaria's tertiary hill region, an important and productive agricultural
 111 landscape in Central Europe. The rolling topography is characterised by predominantly east-facing slopes ranging
 112 from 0.4° to 11.5° (Wilken et al., 2019a). Climate conditions include a mean annual temperature of 8.4 °C and
 113 mean annual precipitation of 834 mm (1994-2001), with the highest precipitation occurring between May and
 114 July (Fiener et al., 2019a). Management practices at the farm follow a comprehensive soil conservation
 115 philosophy based on two main principles: (i) keeping arable soils covered as long as possible and (ii) reducing
 116 hydrological and sedimentological connectivity as far as possible (Fiener et al., 2019a). Within the watersheds,
 117 soils consist predominantly of loamy or silty loamy Cambisols (World Reference Base for Soil Resources (WRB),
 118 Schad et al., 2022).

119 The research area comprises six micro-scale watersheds (W01-W06) with a total area of 24 ha and four
 120 agricultural fields (F15-F18, Fig. 1). The six watersheds exhibit different landscape connectivity characteristics:
 121 W01-W04 (0.8 to 4.2 ha) are classified in this study as field-dominated systems due to their structure, with most
 122 of their area covered by agricultural fields and minimal landscape structures along sediment flux pathways. In
 123 contrast, W05 and W06 are classified as structure-dominated systems due to their configuration, featuring more
 124 complex landscapes. The Watershed W06 (5.7 ha) constitutes the upper part of the larger watershed W05 (7.8
 125 ha) (Fiener et al., 2019a).

126 Three key conservation measures were implemented to minimise hydrological and sedimentological connectivity:
 127 (i) optimised field layout with fields arranged parallel to contour lines, (ii) retention ponds at field borders, and
 128 (iii) a grassed waterway along the main thalweg of W05 and W06. The retention ponds were located at the outlets
 129 of watersheds W01, W02, W05, and W06 (Fig. 1). Sediment trapping efficiency measurements were conducted
 130 for these ponds, revealing an average of 70 ± 14 % (Fiener et al., 2005). Additionally, continuous monitoring
 131 systems were installed at the outlet of each micro-scale watershed to measure runoff and sediment delivery. The
 132 distinction between field-dominated and structure-dominated watersheds will be used consistently throughout
 133 this study.

134 All fields within the watersheds were managed using no-till practices with a crop rotation of winter wheat, maize,
 135 winter wheat, potatoes, whereas the rotation was shifted between the fields (F15-F18, Fig. 1). After winter wheat,
 136 mustard was sown as a cover crop. In the case of potatoes, the mustard was sown into the potato dams built in
 137 autumn, while direct seeding into the down-frozen mustard was performed in the following year.

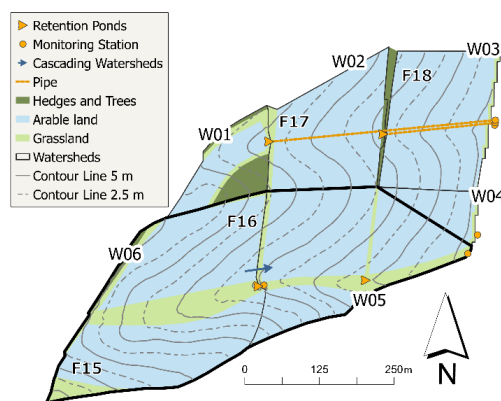


Figure 1: Land use and topography of the experimental farm in Scheyern, Bavaria, with flow direction from west to east.
Note: watershed W05 (thick line) includes the upslope watershed W06.

2.2 Data

The study utilised a unique erosion monitoring dataset acquired between 1994 and 2001. This comprehensive dataset, as well as metadata, are provided by Fiener et al. (2019a). All spatial data were resampled to a consistent 5 m by 5 m grid resolution, matching the digital elevation model (DEM) provided in the dataset (Wilken et al., 2019a). The temporally dynamic input data included daily soil cover measurements and high-resolution precipitation data recorded at 1-minute intervals from up to 11 monitoring sites (Wilken et al., 2019b). Additional details regarding these input parameters are provided in section 2.4 below.

For model testing, we used continuous sediment delivery data from the six micro-scale watersheds between 1994 and 2001. Runoff and suspended-sediment loads were monitored with a measuring system based on a Coshocton-type wheel sampler (precision $\pm 10\%$; Carter and Parsons, 1967; Fiener and Auerswald, 2003). The device continuously diverted an aliquot of approximately 0.5 % from the total flow that left the watersheds through underground-tile outlets with a diameter of 15.6 cm and 29 cm (Fig. 1). At lower rates ($< 0.5 \text{ L s}^{-1}$) the system slightly over-estimated runoff, but these small events contributed negligibly to the cumulative water and sediment budgets. Under sampling during very high flows was avoided by (i) employing large wheels ($\varnothing 61 \text{ cm}$) and (ii) the flow-dampening effect of the retention ponds situated immediately upstream of each outlet (Fiener and Auerswald, 2003).

2.3 Soil erosion modelling

The WaTEM/ SEDEM version used in this study consists of two main components: (i) WaTEM, which implements a spatially distributed German adaption of the USLE, and (ii) SEDEM, which incorporates a transport capacity (TC) equation (Eq. 3) and a routing algorithm for sediment re-distribution based on a DEM (Verstraeten et al., 2002; Van Rompaey et al., 2001; Van Oost et al., 2000). To implement WaTEM/ SEDEM within the GLUE-framework, the original Delphi code-based model was translated to Python 3.12 and was run in PyCharm 2024.1 (Community Edition), which substantially improved computational speed through parallel processing and allowed for easier



164 data handling. Although the Python implementation includes tillage erosion calculations, this component was not
 165 utilised in the present study.

166 The model was applied for the period from April to October of each year from 1994 to 2001, excluding periods
 167 potentially affected by snowmelt erosion and prolonged surface runoff from return flow (Fiener et al., 2019a).
 168 While these months contributed 10.7 % of the total measured sediment delivery (Fiener et al., 2019b), our
 169 analysis focused on the dominant water erosion period during heavy rainfall months. Each micro-scale watershed
 170 was separately modelled.

171 **2.4 Potential Erosion**

172 In contrast to the original WaTEM/ SEDEM (Verstraeten et al., 2002; Van Rompaey et al., 2001; Van Oost et al.,
 173 2000), in which the USLE factors are derived according to the RUSLE approach (Renard, 1997), we calculated the
 174 USLE factors as calculated according to their German adaptation (Eq. 1) (Schwertmann et al., 1987; Din-
 175 Normenausschuss, 2022):

$$176 \quad A = R * K * LS * C * P, \quad (1)$$

177 Where A is the potential erosion ($\text{t ha}^{-1} \text{yr}^{-1}$), R the rainfall erosivity factor in ($\text{N h}^{-1} \text{yr}^{-1}$), K the soil erodibility
 178 factor ($\text{t ha}^{-1} \text{h N}^{-1}$), LS the slope length and steepness factor (dimensionless), C the cover management factor
 179 (dimensionless), and P the agricultural practices factor (dimensionless).

180 The high-resolution rainfall data from eleven (1994–1997) and two (1998–2001) precipitation monitoring stations
 181 located in the research area were used to calculate the rain erosivity factor (R-factor) (Wilken et al., 2019b).
 182 According to the German adaptation of the USLE, rainfall events were considered erosive if they met at least one
 183 of two criteria: (i) total rainfall amount $\geq 10 \text{ mm}$ or (ii) maximum 30-minute intensity $\geq 10 \text{ mm h}^{-1}$. Individual
 184 events were separated by at least 6 hours without rainfall (Schwertmann et al., 1987; Din-Normenausschuss,
 185 2022). The calculated rainfall erosivities per monitoring station were interpolated to 5 m by 5 m resolution maps
 186 using inverse distance weighting, and the spatially distributed values ranged between 65.90 and 155.10 $\text{N h}^{-1} \text{yr}^{-1}$
 187 across the eight-year study period.

188 Soil erodibility (K factor) values were computed following Auerswald et al. (2014) and already provided in the
 189 monitoring data set (Auerswald et al., 2019a). The values, originating from a 50 by 50 m sampling grid, were
 190 spatially interpolated using ordinary kriging to generate a continuous surface with a 5 m by 5 m resolution grid.
 191 The resulting K factor values across the study area ranged from 1.8 to 4.6 $\text{t ha}^{-1} \text{h N}^{-1}$.

192 The slope length and slope steepness factor (LS factor) was calculated based on the DEM using the approach by
 193 Desmet and Govers (1996). When calculating the LS factor for W01, the shrubbed area (Fig. 1) was excluded due
 194 to its negligible runoff contribution. Additionally, we calculated the LS factors for W02 and W03 separately from
 195 their upslope catchments (i.e. W01 and W02), since their runoff was directed via underground pipes to the
 196 monitoring stations (see Fig. 1).

197 The annual crop factor (C factor) was calculated by combining seasonal rainfall erosivity with temporal changes
 198 in soil coverage (Schwertmann et al., 1987). The soil loss ratio (SLR) quantifies the protective effect of soil



coverage by comparing potential soil loss under a given vegetation condition to that under standardised fallow conditions (Schwertmann et al., 1987; Wischmeier and Smith, 1978). While the *SLR* traditionally considers five crop growth stages, from bare soil (0% cover) to full canopy coverage (75-100% cover), we also considered crop residue cover.

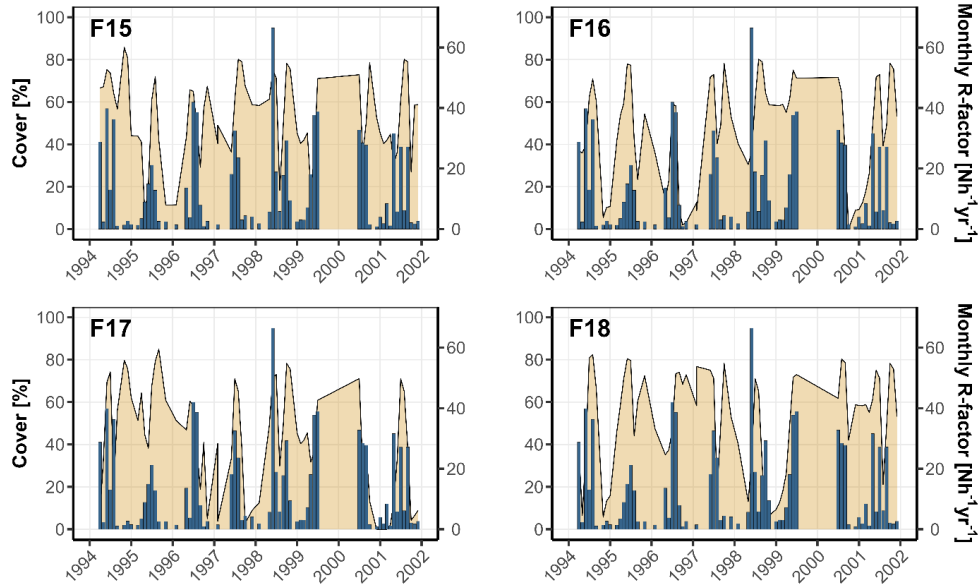
From 1994 to April 1997, direct bi-weekly measurements during growing seasons and monthly measurements during autumn and spring were conducted, with additional observations before and after soil management operations. These field measurements included both crop and residue cover. From these field measurements, standardised daily crop development and residue cover were established and used for the subsequent period from April 1997 onwards (Auerswald et al., 2019b; Fiener et al., 2019a).

Total soil cover was calculated with residues protecting portions of the otherwise exposed soil according to:

$$Co_{tot} = Co_{crop} + (100 - Co_{crop}) * \frac{Co_{res}}{100}, \quad (2)$$

With Co_{tot} is the total soil cover (%), Co_{crop} the cover of the growing crop on the respective field (%), and Co_{res} the measured soil cover of the residues (%).

Figure 2 illustrates the total soil cover on the respective fields with monthly rainfall erosivity. Determining field-specific *SLR* values involved categorising soil cover into the five growth stages and assigning corresponding *SLR* values. As no-till was applied at the research farm, lower *SLR* values were assigned than in conventional systems due to increased soil surface protection. These *SLR* values were obtained from Schwertmann et al. (1987) and adapted based our expert knowledge regarding the soil conservation practices in the Scheyern experimental farm (Fiener and Auerswald, 2007; Fiener et al., 2019a).



218

219 **Figure 2: Each field's total soil cover (Residues and crops). Blue bar plots (monthly sum) show monthly R-factors.**

220 The support practices factor (P factor) was not specifically parametrised for contour-seeding because of field
 221 heterogeneity, i.e. not all parts of a single field were contour-seeded, and/or the absence of specific P factor
 222 values for structures such as the potato dams. However, we accounted for the uncertainty stemming from this
 223 lack of parameter representation as part of the model conditioning process (see section 2.4 below).

224 2.5 Sediment Transport and Deposition

225 The Transport Capacity (TC) quantifies the maximum amount of sediment transported through a grid cell without
 226 deposition. When the incoming sediment load into a raster cell exceeds TC , the excess material is deposited within
 227 the cell, whilst the remaining portion continues its downstream movement. TC was calculated with the approach
 228 proposed by Van Rompaey et al. (2001):

$$229 \quad TC = k_{TC} * R * K * (LS - S_{IR}), \quad (3)$$

230 with:

$$231 \quad S_{IR} = 4.12 * S_m^{0.8} \quad (4)$$

232 where TC is the transport capacity ($t \, ha^{-1}$), k_{TC} the transport capacity coefficient (m) described below, R the
 233 rainfall erosivity factor in ($N \, h^{-1} \, yr^{-1}$), K is the soil erodibility factor ($t \, ha^{-1} \, h \, N^{-1}$), LS the slope length and steepness
 234 factor (dimensionless), S_{IR} the interrill slope gradient factor (dimensionless) and S_m the slope ($m \, m^{-1}$).

235 The transport capacity coefficient (k_{TC}) represents the theoretical upslope distance required for sediment
 236 generation to reach maximum TC at a given raster cell under the assumption of uniform slope and erosion
 237 conditions (Van Rompaey et al., 2001). The transport capacity coefficient depends on surface roughness and



238 therefore differs according to land use and management. In our model parameterisation, we distinguish between
 239 higher values for arable ($k_{TC/A}$) land and lower values for grassland ($k_{TC/G}$; along field borders and in grassed
 240 waterways).

241 WaTEM/SEDEM's hillslope sediment transport module employs a multiple flow routing algorithm, which
 242 distributes sediment from individual cells to their downslope neighbours based on Quinn et al. (1991). The
 243 algorithm calculates local slopes to eight neighbouring cells and applies specific weighting factors: 0.50 for
 244 orthogonal neighbours and 0.35 for diagonal neighbours. The sediment flux is distributed proportionally to the
 245 weighted slope values of all cells at equal or lower elevations.

246 In this study, we implemented the Parcel Connectivity (p_{con}) parameter specifically at field boundaries. p_{con}
 247 reduces the contributing upstream area by a value [%] at these transitions (Notebaert et al., 2006). This reduction
 248 has a dual effect: (i) it directly lowers the slope length part of the LS factor, thereby decreasing the potential
 249 erosion for subsequent downstream cells, and (ii) it affects the TC, which is calculated using the LS factor (Eq. 3).
 250 Unlike the original WaTEM/SEDEM version (Notebaert et al., 2006), we implemented p_{con} within the multiple flow
 251 routing algorithm loop calculating the contributing upstream area, ensuring its effects propagate downstream
 252 through the flow network. Consequently, the reduction in sediment transport influences the downstream cells
 253 and extends to subsequent agricultural fields and vegetated areas. Moreover, we introduced a border deposition
 254 (b_{dep}) parameter, which represents a forced deposition mechanism activated when agricultural field cells
 255 contribute sediment to adjacent vegetated areas. Under these conditions, a defined percentage of the
 256 transported sediment is deposited directly at the field border within the field.

257 Retention ponds were implemented within the 5 m by 5 m land use raster map. The locations of the four retention
 258 ponds at the outlets of the micro-scale watersheds were mapped, with assigned trapping efficiencies of 54 %, 82
 259 %, 59 %, and 85 % for watersheds W01, W02, W05, and W06, respectively, as measured in Fiener et al. (2005).
 260 The standard deviation across all watersheds (± 13.7 %) was applied to account for measurement error in the
 261 trapping efficiency values.

262 **2.6 Generalised Likelihood Uncertainty Estimation (GLUE) framework**

263 We employed the GLUE methodology (Beven and Binley, 1992) to represent model and measurement
 264 uncertainties and to identify and analyse behavioural parameter sets. The GLUE approach recognises that
 265 multiple parameter sets may provide equally acceptable simulations of a system within the limitations of a given
 266 model structure and observational errors (Beven, 2006).

267 We established limits of acceptability for the simulated sediment yields by considering multiple sources of
 268 uncertainty in the event-based measurements of runoff and sediment concentrations used for calculating annual
 269 and median annual sediment yields. These included Coshocton wheel measurement errors (± 10 %, Fiener and
 270 Auerswald, 2003), runoff collector barrel sampling errors (estimated ± 10 %), and retention pond uncertainties (\pm
 271 14 %). For events with data collection issues (flagged in the data set), we assigned an additional ± 50 % error
 272 margin. However, for events flagged as "barrels overflow", we introduced only an upper error boundary since
 273 the measurement taken from the barrel represents a minimum possible sediment yield during a rainfall event.



274 Finally, we propagated the measurement errors using a Monte Carlo simulation with 1,000 realisations and
 275 sampling from normal distributions that represented the range of potential errors. The 2.5th and 97.5th percentiles
 276 of the resulting aggregated (annual and median annual) sediment yields were used as the limits of acceptability
 277 for simulated values. These uncertainty bounds served as criterion for behavioural model realisations. Hence,
 278 only simulations producing outputs within these error margins were classified as behavioural and retained for
 279 subsequent analysis.

280 2.7 Model evaluation

281 The model results were evaluated using R-Studio (R 4.4.2; R-Studio 2024.12.1 Build 563) in two phases to account
 282 for the different sediment transport processes in field-dominated and structure-dominated watersheds.

283 Phase 1 - Field-dominated watersheds:

284 We performed a Monte Carlo simulation with 25,000 realisations for the field-dominated watersheds, sampling
 285 parameters from uniform distributions across *a priori* selected ranges (Tab. 1). To consider the inherent potential
 286 errors in USLE calculations, including uncertainties associated with the parameterisation of the P factor, we
 287 modified the potential erosion in individual raster cells through an error surface (e_{sur}) before routing the
 288 sediment. This error surface was sampled from a uniform distribution for each realisation, modifying the USLE-
 289 calculated potential erosion (Eq. 1) within a range of 0 to ± 0.5 :

$$290 A_{new,i} = A_i + A_i * e_{sur}, \quad (5)$$

291 Where A_i is the potential soil erosion ($t\ ha^{-1}\ yr^{-1}$) calculated by the USLE (Eq. 1) at raster cell i , $A_{new,i}$ is the
 292 potential soil erosion ($t\ ha^{-1}\ yr^{-1}$) with incorporated uncertainty at raster cell i , and e_{sur} the error surface
 293 (dimensionless).

294 To ensure that $k_{TC/G}$ is consistently lower than $k_{TC/A}$, both were sampled with a constrained relationship, where
 295 $k_{TC/A}$ values were required to be at least 1.5 but no more than 5 times higher than $k_{TC/G}$ values. Model runs were
 296 classified as behavioural if the simulated sediment yield values fell within the established limits of acceptability
 297 for the observed data. For these behavioural simulations, we calculated likelihoods by rescaling the mean
 298 absolute error (MAE) (Brazier et al., 2000):

$$299 L_i = \frac{1}{MAE_i} / \sum \frac{1}{MAE_i}, \quad (6)$$

300 with:

$$301 MAE_i = |Sim_i - Obs_i|, \quad (7)$$

302 where L_i is the likelihood of one realisation i (dimensionless), MAE_i is the mean absolute error of realisation i ($t\ ha^{-1}\ yr^{-1}$), Sim_i is the simulated values for behavioural runs of realisation i ($t\ ha^{-1}\ yr^{-1}$), and Obs_i is the observed
 303 sediment value for realisation i ($t\ ha^{-1}\ yr^{-1}$).
 304



Table 1: Parameter ranges used for MC simulation in the WaTEM/SEDEM model. These ranges were selected based on the literature on previous model applications. $k_{TC/A}$ and $k_{TC/G}$ are the transport capacity coefficients for arable land and grassland, p_{con} is the parcel connectivity, e_{sur} is the error surface and b_{dep} the border deposition.

Range	$k_{TC/A}$ [m]	$k_{TC/G}$ [m]	p_{con} [%]	e_{sur}	b_{dep} [%]
low	1	1	50	-0.5	0
high	300	100	90	0.5	20

Phase 2 - Structure-dominated watersheds:

For the structure-dominated watersheds, we used the likelihoods associated with behavioural parameter values conditioned in Phase 1 to represent in-field processes ($k_{TC/A}$ and e_{sur}) in order to generate another model 25,000 realisations. In this second phase, the model conditioning was focused on the parameters controlling sediment redistribution through landscape structures ($k_{TC/G}$, b_{dep} and p_{con}). The same limits of acceptability approach as in phase one was applied to identify behavioural simulations. We calculated new likelihood values for these simulations to analyse their performance in representing structural erosion control measures.

2.8 Spatiotemporal model evaluation

Model outputs were analysed at multiple spatiotemporal scales through sequential aggregation steps: First, we calculated an eight-year median of the sediment yield for each individual watershed. Second, we spatially aggregated the watersheds based on their dominant erosion characteristics (field- and structure-dominated) while maintaining an annual resolution. Third, we aggregated the median values over the eight-year monitoring period for these spatially aggregated groups.

To further analyse relative errors, the percent bias ($PBIAS$) was calculated by:

$$PBIAS = \left(\frac{Sim_i - Obs_i}{Obs_i} \right) * 100, \quad (8)$$

Where Sim_i is the simulated values for behavioural realisation i ($t \text{ ha}^{-1} \text{ yr}^{-1}$), and Obs_i is the observed sediment value for realisation i ($t \text{ ha}^{-1} \text{ yr}^{-1}$).

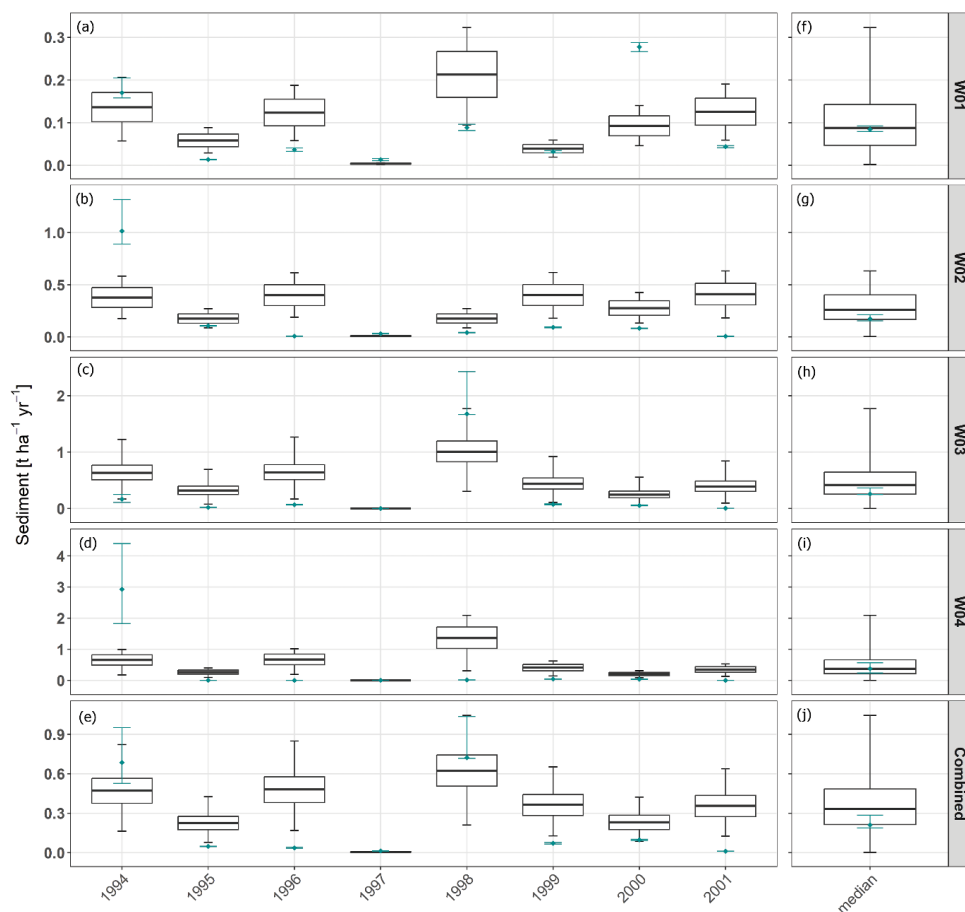
3. Results

3.1 Model Performance Across Scales

The annual model results for field-dominated watersheds (W01-W04) were within the same order of magnitude of the measured sediment yields. However, the model was not considered behavioural for predicting annual sediment yields according to our pre-established acceptability criterion. The simulated annual sediment yields were predominantly overestimated (22 out of 32 cases; Fig. 3a-d), occasionally underestimated (3 out of 32 cases, i.e. in the year 2000 in W01; 1994 in W02; 1994 in W04; Fig. 3a, b and d), with only a small portion of simulations meeting our acceptability criterion (7 out of 32 cases; Fig. 3a-d). The tendency to overestimate sediment yield is more pronounced in watersheds W05 and W06. Only in 1994 the model underestimated measured sediment



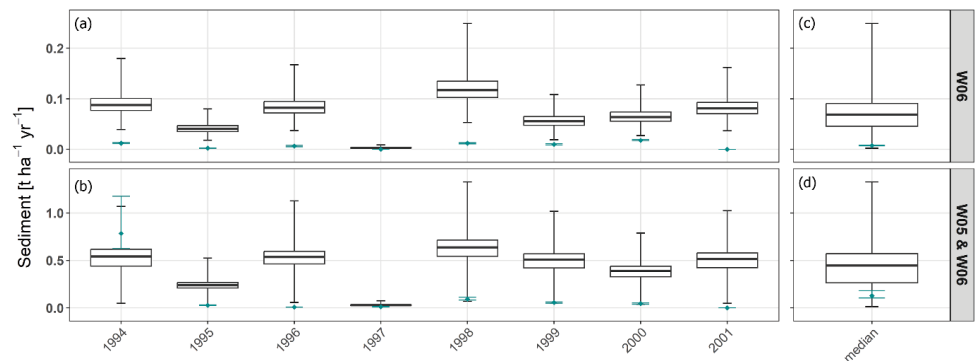
334 yields in watershed W05 (Fig. 4b). In W06, measured sediment yields were the lowest among all watersheds
 335 (maximum of $0.02 \text{ t ha}^{-1} \text{ yr}^{-1}$ in 2000), with zero sediment yield measurements in 1995, 1997, and 2001, yet the
 336 model consistently overestimated sediment yield across all years in this watershed.



337

338 **Figure 3: Annual and eight-years median sediment yields in field-dominated watersheds. (a-d) Box plots display the median,**
 339 **1. and 3. quartile and the full range of simulated sediment yields from 25,000 model realisations with different parameter**
 340 **sets (black whiskers), while median sediment yield measurements are shown as blue dots with computed error ranges**
 341 **(cyan whiskers). (f-i) The watershed-specific 8-year median measured yield with error ranges and simulated yields. (e)**
 342 **Annual spatially combined watershed sediment yields. (j) 8-year median of spatially aggregated watersheds.**

343 When evaluated using eight-year median values, model performance showed better agreement with
 344 observations. The eight-year median modelled sediment yield across field-dominated watersheds (W01-W04)
 345 was $0.24 \text{ t ha}^{-1} \text{ yr}^{-1}$, closely aligning with the measured eight-year median of $0.21 \text{ t ha}^{-1} \text{ yr}^{-1}$. For structure-
 346 dominated watersheds W05 and W06, we simulated an eight-year median of $0.15 \text{ t ha}^{-1} \text{ yr}^{-1}$ (Fig. 4c, d), against a
 347 measured median of $0.13 \text{ t ha}^{-1} \text{ yr}^{-1}$. The 1994 sediment yield peak in W05 strongly influenced the system's overall
 348 performance, ultimately leading to an increased number of behavioural model realisations when evaluated across
 349 the entire period (Fig. 4d).



350

351 **Figure 4: Annual and eight-years median sediment yields in structure-dominated watersheds. (a-b) Box plots display the**
352 **median, 1. and 3. quartile and the full range of simulated sediment yields from 25,000 model realisations with different**
353 **parameter sets (black whiskers), while median sediment yield measurements are shown as blue dots with computed error**
354 **ranges (cyan whiskers). (c-d) The watershed-specific 8-year median measured yield with error ranges and simulated yields.**

355 The eight-year temporal aggregation revealed varying proportions of behavioural model realisations across
356 individual watersheds. W04 had the highest amount with 57 % of all realisations, while other watersheds
357 exhibited lower proportions (W01: 13 %, W02: 21 %, W03: 23 %). W05 exhibited minimal behavioural realisations
358 of 1 %. Although the range of our simulated values overlapped with the error margins for the measured sediment
359 yields in W06 (Fig. 4c), none of the actual model realisations matched the observational data including
360 measurement errors. Furthermore, no common behavioural realisations were found across all watersheds,
361 indicating that each watershed had a different behavioural parameter space.

362 The analysis of the spatially aggregated watersheds (field-dominated vs. structure-dominated), while maintaining
363 annual temporal resolution, revealed behavioural model realisations in some years but not consistently
364 throughout the entire eight-year period for each watershed group (Fig. 3e, 4b). When combining both spatial and
365 temporal aggregation, behavioural realisations were generated for each watershed group (Fig. 3j, 4d). Across the
366 entire set of 25,000 realisations, the median MAE values were 0.12 t ha⁻¹ yr⁻¹ for field-dominated watersheds and
367 0.16 t ha⁻¹ yr⁻¹ for structure-dominated watersheds, with maximum MAE values of 0.34 t ha⁻¹ yr⁻¹ and 0.39 t ha⁻¹
368 yr⁻¹, respectively. Table 4 presents the model performance metrics specifically for the subset of behavioural model
369 realisations within the watershed groups.

370

371

372

373



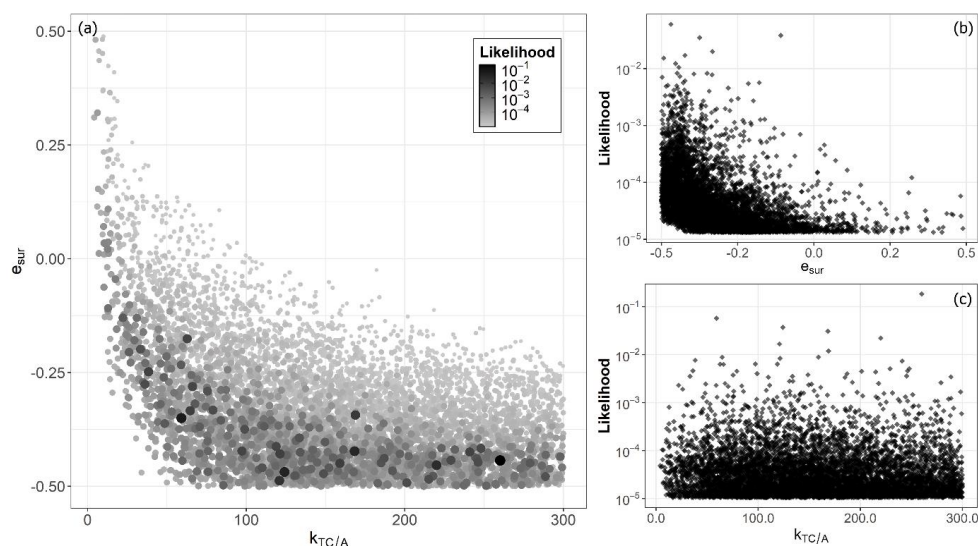
374 **Table 2: Comparison of model performance metrics between micro-scale watershed groups based on eight-year median of**
 375 **behavioural realisations, including median sediment yield (SY) as well as error statistics (MAE, PBIAS) with maximum**
 376 **(Max.), median (Med.) and minimum (Min.) values.**

Unit of measure		Field-dominated	Structure-dominated
Behavioural realisations [%]		30.04	1.33
Measured SY [t ha ⁻¹ yr ⁻¹]	Med.	0.21	0.13
Simulated SY [t ha ⁻¹ yr ⁻¹]	Med.	0.24	0.15
MAE [t ha ⁻¹ yr ⁻¹]	Min.	4.21*10 ⁻⁶	5.76*10 ⁻⁵
	Med.	0.03	0.03
	Max.	0.07	0.05
PBIAS [%]	Min.	-10.79	-17.70
	Med.	15.35	20.15
	Max.	35.38	42.64

377 3.2 Behavioural parameter space

378 We analysed the behavioural parameter space for the spatially and temporally aggregated watershed groups, as
 379 only this aggregation level yielded behavioural realisations for both field-dominated and structure-dominated
 380 watershed groups.

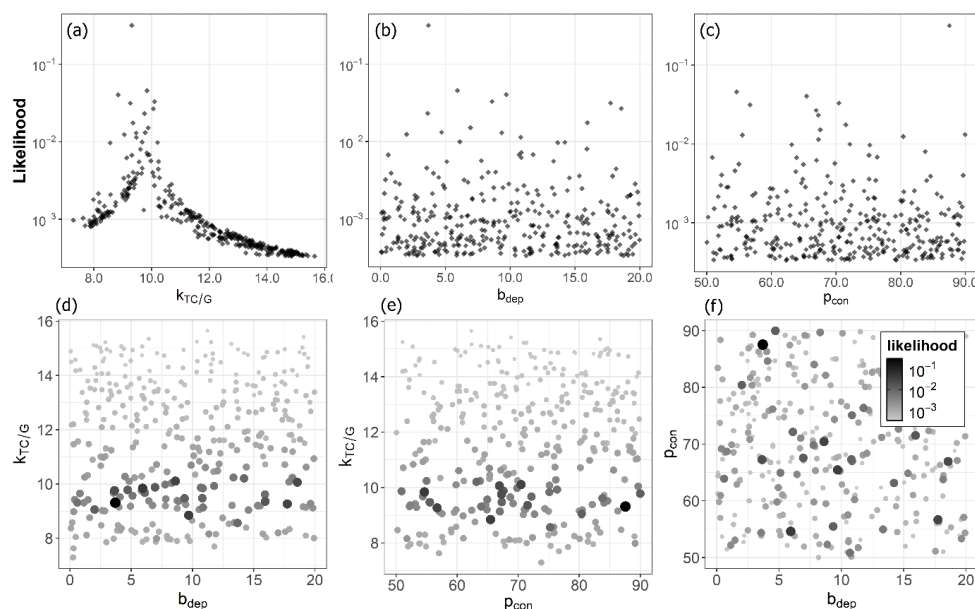
381 For field-dominated watersheds, the analysis focused on the error surface and in-field parameter e_{sur} and $k_{TC/A}$.
 382 While behavioural realisations were identified across the entire ranges of all parameters, higher likelihood values
 383 concentrated in specific regions. Specifically, e_{sur} values closer to -0.5 exhibited higher likelihood values than lower
 384 e_{sur} values (Fig. 5b). In contrast, $k_{TC/A}$ showed no discernible pattern across the response surface (Fig. 5c). The
 385 relationship between these parameters revealed a clear compensation mechanism, where lower $k_{TC/A}$ values
 386 required higher s_{cor} values to produce behavioural realisations (Fig. 5a).



387

388 **Figure 5: Parameter likelihoods across field-dominated micro-scale watersheds, showing only behavioural model**
 389 **realisations. (a) The relationship between e_{sur} and $k_{TC/A}$ parameters. Circle size and shade intensity indicate the likelihood**
 390 **of each parameter combination, with larger and darker circles representing higher likelihood values. (b) The relationship**
 391 **between likelihood and e_{sur} . (c) The relationship between likelihood and $k_{TC/A}$.**

392 In structure-dominated watersheds, the analysis focused on parameters controlling sediment transportation and
 393 deposition in grassland ($k_{TC/G}$, b_{dep} , and p_{con}). The $k_{TC/G}$ parameter exhibited a distinct likelihood peak between
 394 approximately 9 and 11 m, with behavioural values ranging from approximately 7.5 m to 15 m (Fig. 6a), which is
 395 notably narrower than the sampled range of up to 150 (Tab. 1). In contrast, b_{dep} and p_{con} showed no sensitivity,
 396 displaying relatively uniform likelihood distributions across their entire ranges (Fig. 6b, c). When plotting b_{dep}
 397 against p_{con} , homogeneous likelihood distributions emerged with no apparent dependencies (Fig. 6f).
 398 Examinations of b_{dep} and p_{con} against $k_{TC/G}$ revealed a horizontal band of high likelihood values at specific $k_{TC/G}$
 399 values, without any directional trends (Fig. 6d, e).



400

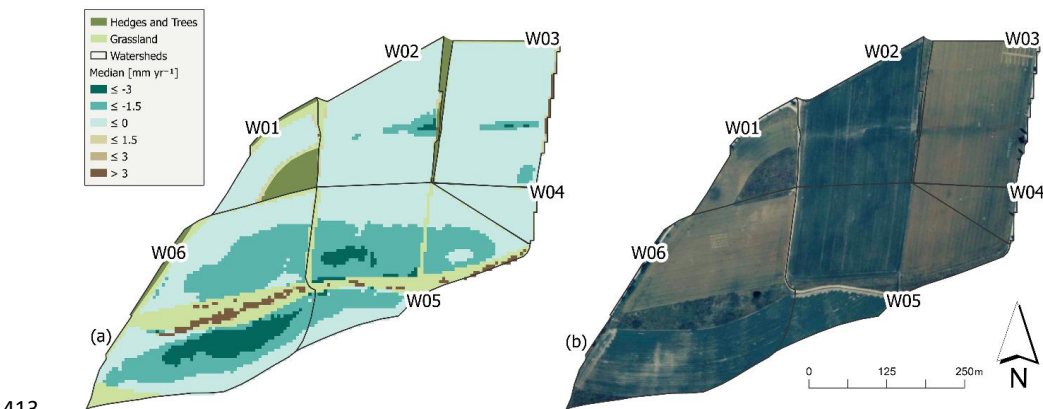
401 **Figure 6: Parameter likelihoods across structure-dominated micro-scale watersheds, showing only behavioural model**
 402 **realisations. (a) The relationship between likelihood and $k_{TC/G}$. (b) The relationship between likelihood and b_{dep} . (c) The**
 403 **relationship between likelihood and p_{con} . (d) The relationship between b_{dep} and $k_{TC/G}$. Circle size and colour intensity indicate**
 404 **the likelihood of each parameter combination, with larger and darker circles representing higher likelihood values. (e) The**
 405 **relationship between p_{con} and $k_{TC/G}$. (f) The relationship between b_{dep} and $k_{TC/G}$.**

406 3.3 Spatial analysis

407 In field-dominated watersheds, substantial deposition was primarily confined to retention ponds, while other
 408 areas outside arable lands showed relatively minimal deposition, as shown in the 50th percentile (median) of
 409 behavioural model realisations (Fig. 7a). In W04, negligible to no deposition was observed. Conversely, structure-
 410 dominated watersheds exhibited considerably more intense erosion-deposition dynamics. The grassed waterway



411 showed a clear deposition pattern, with W06 exhibiting the most pronounced deposition patterns leading toward
412 the retention pond at the outlet of W06.



413
414 **Figure 7: (a) The median of simulated potential erosion and deposition of behavioural model realisations over the eight-**
415 **year period. (b) An aerial photograph of the study area shows the land use patterns and field boundaries on the Scheyern**
416 **experimental farm in 2002.**

417 4. Discussion

418 4.1 GLUE Framework and Uncertainties

419 We tested WaTEM/SEDEM using a limits of acceptability approach within the GLUE framework. For this, we
420 implemented a two-phase approach, first conditioning and evaluating field-dominated watersheds, and then
421 using the behavioural parameter space of these watersheds to condition and evaluate structure-dominated
422 systems. Alatorre et al. (2010) demonstrated that soil erosion models often exhibit parameter compensation
423 effects, where different parameter combinations produce similar outputs at the catchment scale - a manifestation
424 of the equifinality concept (Beven, 2006). Our sequential approach helped to minimise these effects by first
425 constraining the simulated erosion ($k_{TC/A}$ and e_{sur}) in field-dominated watersheds and then conditioning the
426 transport parameters ($k_{TC/G}$, p_{con} and b_{dep}) in more complex systems.

427 The limits of acceptability approach incorporated multiple sources of measurement uncertainty. Nearing (2000)
428 demonstrated through replicated plot studies that natural variability in erosion measurements is particularly
429 pronounced for low-magnitude erosion events, such as the ones observed in this study. While Nearing (2000)
430 proposed a quantitative method for estimating the expected variability of erosion measurements, his approach
431 is specifically developed for plot-scale studies and cannot be extrapolated to watersheds or more complex
432 landscape systems. Given the (to the best of our knowledge) current absence of methodologies for determining
433 error boundaries for low sediment yield measurements at larger scales, we necessarily relied on relative error
434 estimates. An implementation of proper measurement variability-derived error ranges would likely result in a
435 substantially higher number of behavioural model realisations, particularly for low sediment yield measurements
436 where the variability is the highest (Nearing, 2000). This reveals the need for developing robust approaches for



defining limits-of-acceptability criteria for sediment yield estimates that account for the full range of uncertainties, e.g. instrument precision, sampling errors, data processing, or site-specific variations.

Erosion models typically exhibit systematic biases, overpredicting low sediment yields while underpredicting high sediment yields (Nearing, 1998; Risse et al., 1993; Kinnell, 2007). This is particularly relevant for our study area, where the median measured sediment yield of $0.16 \text{ t ha}^{-1} \text{ yr}^{-1}$ was substantially lower than erosion rates which can exceed $10 \text{ t ha}^{-1} \text{ yr}^{-1}$ in the Bavarian Tertiary hill region (Auerswald et al., 2009). To investigate the modelling under/over prediction issue, we used an error surface (e_{sur}) multiplied with the erosion calculated by the USLE (Eq. 5). The e_{sur} parameter served three purposes: (i) adjusting potential erosion to investigate the USLE's inherent biases, (ii) analysing the biases by looking at the behaviour of e_{sur} , and (iii) representing the uncertainty stemming from measurement errors for the USLE factors and the lack of parameterisation for the P factor. The analysis of behavioural model realisations revealed a concentration of likelihood values near small e_{sur} values, reducing sediment by up to 50 % (Fig. 5b). This indicates that in our study WaTEM/SEDEM overestimates soil erosion in landscapes with implemented conservation measures. This is also evident looking at figure 3a-d and 4a-b, which illustrate a general tendency for overestimation of modelled sediment yields in all watersheds.

4.2 Model Performance and Limitations

WaTEM/SEDEM correctly simulated the magnitude of the very low sediment yields in micro-scale watersheds under optimized soil conservation, with annual values closely aligning with measured data (Fig. 3a-d, 4a-b). Despite this achievement, the model did not consistently meet our strict limits of acceptability for annual realisations and therefore was rejected for making precise annual simulations. However, the model's performance improved notably when applied to longer-term medians and larger spatial units, where more behavioural model realisations were identified.

Field-dominated watersheds

The model simulated the very low sediment yields resulting from well-established in-field soil conservation practices in field-dominated watersheds, comparable to the measured data. In general, observed sediment yields were overestimated, which can be attributed primarily to difficulties in accurately representing the specific C factors of this conservation system, particularly unique practices such as mustard sown onto autumn-built dams where potatoes were later directly planted (Fiener and Auerswald, 2003). Such unconventional approaches are not adequately captured in the *SLR* values for no-till systems as evaluated in the German adaptation of the USLE (ABAG; Schwertmann et al., 1987; Naw, 2022), even with the use of very low soil loss ratios in the parameterisation of the C factor, which represent the continuous soil cover through the crop rotation in the experimental farm (Fig. 2).

Conversely, the model underestimated sediment yields in some years because even optimally managed conservation systems experience short time windows with weak protection. During these short windows with reduced soil protection (Fig. 2), substantial erosion events may occur, like in systems not under soil conservation. In general, erosion processes are typically dominated by extreme events (Gonzalez-Hidalgo et al., 2012; Steegen et al., 2000), as exemplified in our study by an April 1994 rainfall event of 114 mm within 66 hours coinciding with



low soil coverage in W02 (Fig. 2), accounting for approximately 58 % of that year's total sediment yield (see year 1994 in Fig. 3b). The model's annual time step fails to capture these critical temporal coincidences, a limitation that becomes more pronounced when such events are infrequent. This temporal limitation aligns with findings by Risse et al. (1993), who demonstrated that USLE's model efficiency diminishes at the annual scale. When averaging over the eight-year study period, these extreme events are smoothed out, which explains the model's improved performance at longer timescales (Tab. 2). This observation supports the basic assertion that the USLE was designed to compute long-term soil losses (Wischmeier and Smith 1978).

For the temporally aggregated eight-year medians, there was no single parameter set that produced behavioural model realisations across all field-dominated watersheds simultaneously when applying our limits of acceptability criterion. This indicates a limitation in parameter transferability within our study context. While Van Rompaey et al. (2001) recognized technical limitations of WaTEM/SEDEM in model transferability related to grid size and routing methods, our findings suggest additional challenges in accurately representing processes within micro-scale conservation landscapes. The need for watershed-specific calibration, even within relatively homogeneous landscapes with similar crop and soil properties, indicates that parameter calibration compensates for inherent model or data limitations. At such fine scales, WaTEM/SEDEM may struggle to accurately represent the complex interactions between soil conservation measures and erosion processes.

Similar calibration challenges seem to exist more broadly in WaTEM/SEDEM applications across different landscape types and research questions, as evidenced by a wide range of calibrated k_{TC} values reported across different studies (Tab. 3), with $k_{TC/A}$ values varying from 10 to 174.4 m. As Beven (2006) argues, such calibration approaches may achieve mathematical fitting while concealing fundamental model inadequacies.

493 **Structure-dominated watersheds**

Unlike field-dominated watersheds, structure-dominated systems demonstrated different response patterns to extreme erosion events. In these watersheds, sediment generated during individual large erosion events (as observed in the field-dominated watersheds), is predominantly captured by grassed waterways and retention ponds (Fiener and Auerswald, 2003, 2005), thus reducing the variability of event sediment yields. This buffering effect explains why the model consistently overestimates sediment yield across all years for structure-dominated watersheds (Fig. 4a-b), in contrast to the occasional underestimation observed in field-dominated systems (Fig. 3a-d).

Only one exception to this pattern was observed: the model underestimated sediment yield in W05 during 1994, when the lower part of the grassed waterway required reseeding after losing its initial grass cover along the thalweg during a spring erosion event (Fiener and Auerswald, 2003). This exceptional case quantitatively demonstrates the role of functional grassed waterways, as the measured sediment yield in 1994 for W06 was substantially higher ($0.78 \text{ t ha}^{-1} \text{ yr}^{-1}$) than in subsequent years when the grassed waterway was fully established (averaging only $0.03 \text{ t ha}^{-1} \text{ yr}^{-1}$ from 1995-2001), representing an approximately 96 % reduction in sediment yield (Fig. 4b).



508 The model's systematic overestimation of sediment yields in structure-dominated watersheds reveals limitations
 509 in representing the sediment trapping mechanisms of grassed waterways. The primary limitation is the model's
 510 inability to capture re-infiltration processes within the grassed waterway, which is not accounted for in
 511 WaTEM/SEDEM's transport capacity formulation. Fiener and Auerswald (2005) demonstrated that grassed
 512 waterway effectiveness depends strongly on morphological characteristics, particularly the cross-sectional shape,
 513 with flat-bottomed waterways showing substantially higher runoff reduction. The infiltration increases with
 514 length and flatter cross-section of grassed waterways, which provide larger runoff widths and consequently
 515 greater infiltration areas. A previous study showed that in the upper part of the grassed waterway (W06), where
 516 WaTEM/SEDEM more substantially underestimates the sediment trapping, the long-term runoff and sediment
 517 yield reduction was about 90% and 97%, while it was about 10% and 77% in the lower part of the grassed
 518 waterway (W05) with a ditch-like cross-section (Fiener & Auerswald, 2003).

519 4.3 Distribution of behavioural model parameter values

520 The TC within agricultural fields is primarily controlled by a high transport coefficient $k_{TC/A}$ (Van Rompaey et al.,
 521 2001). Lower $k_{TC/A}$ values reduce TC , promoting in-field deposition and consequently decreasing sediment yield
 522 at the watershed outlet. Our analysis revealed behavioural model realisations across the full *a priori* selected
 523 range of $k_{TC/A}$ values, with no clear pattern for field-dominated watersheds, demonstrating no sensitivity even at
 524 very low $k_{TC/A}$ values near 1 or very high e_{sur} values of 0.5 (Fig. 5a). This lack of sensitivity may be attributed to the
 525 implementation of retention ponds in W01 and W02 and by the very low simulated erosion values, as TC
 526 remained sufficiently high to transport the generally low sediment fluxes even with very low $k_{TC/A}$ values.

527 The low transport capacity coefficient for rougher surfaces, in case of this study for grassland $k_{TC/G}$, usually triggers
 528 deposition in these areas (Van Rompaey et al., 2001). Our analysis identified behavioural values for $k_{TC/G}$ between
 529 approximately 7.5 m to 15 m with a notable likelihood spike between approximately 9 m and 11 m, relatively low
 530 values compared to other studies (Tab. 3). While Onnen et al. (2019) reported similarly low values for Danish
 531 landscapes, they explicitly attributed this to sandy soils in Denmark. However, our study area features
 532 predominantly silt loam and loamy soils, which are much more comparable to the Belgian soils (Tab. 3) where
 533 low k_{TC} values for rough surfaces were implemented (Peeters et al., 2008; Verstraeten et al., 2002; Van Rompaey
 534 et al., 2001).

535 **Table 3: Comparison of k_{TC} parameter values of behavioural model realisations used in different studies with**
 536 **WaTEM/ SEDEM.**

High k_{TC} values mostly used for arable land [m]	Low k_{TC} values mostly used for non-arable land [m]	Country	Source
150	not used	Germany	Wilken et al. (2020)
10 to 24	1 to 12	Denmark	Onnen et al. (2019)
100 & 150	25	Belgium	Peeters et al. (2008)
75	42	Belgium	Verstraeten et al. (2002)
75	42	Belgium	Van Rompaey et al. (2001)
174.4	not used	Belgium	Van Oost et al. (2000)

537



538 These low $k_{TC/G}$ values can have some possible interpretations: (i) most likely, the model is compensating for its
 539 inability to represent re-infiltration processes in grassed waterways, and/or (ii) the model may partly compensate
 540 for an overestimation of erosion rates in the draining fields. However, although the model outputs are fully
 541 spatially distributed (Fig. 7a), it is not possible to compare the simulated patterns with spatially distributed
 542 observational data (e.g. aerial images, field surveys), because, except for some rare larger events, the effective
 543 soil conservation established prevents visible erosion features like rills.

544 In our study, WaTEM/SEDEM showed no sensitivity to parameters b_{dep} and p_{con} that represent the influence of
 545 linear landscape features. These parameters displayed homogenous likelihood distributions across the sampled
 546 parameter space (Fig. 6b-c). This lack of sensitivity could stem from several factors: (i) sampling an overly narrow
 547 parameter space, (ii) limited influence of field borders in the studied watersheds due to the layout of the fields
 548 and watersheds with a small number of border situations, and/or (iii) a dominance of $k_{TC/G}$ implemented over a
 549 long grass structure, which may nullify the influence of b_{dep} and p_{con} in the model outputs, especially in watershed
 550 W05 and W06.

551 An additional limitation of the current parameterisation approach is its static nature. The effectiveness of grassed
 552 waterways and retention structures varies throughout the year due to seasonal vegetation changes (Fiener and
 553 Auerswald, 2003). Additionally, there is an important interaction between sediment influx and trapping
 554 efficiency—as influx increases, the relative trapping efficiency typically decreases (Dermisis et al., 2010; Fiener
 555 and Auerswald, 2018). Dermisis et al. (2010) demonstrated this inverse relationship, showing that grassed
 556 waterway trapping efficiency decreases as peak runoff discharge increases, with notable breakpoints in efficiency
 557 between different flow rates. The current static connectivity and transport capacity parameters (p_{con} , b_{dep} and
 558 $k_{TC/G}$) cannot adequately capture these temporal variations and flux-dependent relationships, suggesting the need
 559 for a more dynamic parameterisation approach that accounts for both seasonal changes and influx response.

560 5. Conclusion

561 We evaluated WaTEM/SEDEM's capability to simulate sediment yields in micro-scale watersheds under optimised
 562 soil conservation practices using a limits-of-acceptability approach within the GLUE framework. Our investigation
 563 examined model performance across different levels of spatiotemporal data aggregation and analysed the
 564 sensitivity of the model's response surface to the variability in the behavioural parameter space. Moreover, we
 565 used a two-step conditioning process, in which model parameters linked to in-field erosion processes were
 566 conditioned in field-dominated watersheds and later applied in structure-dominated watersheds, for which a
 567 separate set of connectivity parameters was also conditioned.

568 The model was unable to produce behavioural realisations at annual timesteps based on our strict limits of
 569 acceptability criterion despite the small absolute prediction errors (eight-year $MAE = 0.12 \text{ t ha}^{-1} \text{ yr}^{-1}$ for field-
 570 dominated and eight-year $MAE = 0.16 \text{ t ha}^{-1} \text{ yr}^{-1}$ for structure-dominated watersheds). For the field-dominated
 571 watersheds, the model particularly struggled with the simulation of annual sediment yields when individual
 572 extreme events dominated the annual sediment production.



573 Aggregating model outputs in time and space worked best for field-dominated systems, which compensated for
 574 the underestimation of soil conservation in controlling soil erosion and the model's inability to capture extreme
 575 events within an annual time step. This finding confirms that WaTEM/SEDEM is better suited for long-term
 576 conservation planning than for making precise annual sediment yield predictions in areas with soil conservation
 577 practices.

578 The GLUE framework revealed specific patterns in the sampled parameter space, particularly the compensation
 579 mechanism between $k_{TC/A}$ and e_{sur} values for field-dominated watersheds, and the narrow behavioural parameter
 580 range of $k_{TC/G}$ values (7.5-15 m) for structure-dominated watersheds. The likelihood distributions of $k_{TC/A}$ and
 581 especially e_{sur} enabled the pre-conditioning of structure-dominated watersheds, reducing parameter
 582 compensation effects that typically mask model structural deficiencies.

583 Ultimately, our study demonstrates that WaTEM/SEDEM can simulate the very low sediment yields observed
 584 from soil conservation agricultural systems, provided that high spatiotemporal resolution input data and locally
 585 adapted USLE factors (e.g., the ABAG for Southern Germany) are available. However, capturing the effects of
 586 linear landscape features like grassed waterways where concentrated runoff occurs remains challenging for
 587 WaTEM/SEDEM, primarily due to the model's inability to represent re-infiltrating processes that are critical for
 588 sediment trapping in such structures. Additionally, our model evaluation approach revealed that model
 589 performance strongly depends on the spatiotemporal scale of analysis. While the model produced behavioural
 590 realisations for the aggregated eight-year monitoring period, it did not reliably simulate annual sediment yields.
 591 For long-term, large-scale soil conservation planning in which the effects of single erosive events on individual
 592 fields are less relevant for representing the system behaviour, WaTEM/SEDEM is fit for purpose.

593 **Code availability**

594 The code is available on reasonable request.

595 **Data availability**

596 The input data are openly available and can be downloaded here:
 597 <https://adgeo.copernicus.org/articles/48/31/2019/adgeo-48-31-2019.html> (Last visited 11.07.2025)

598 **Author contribution**

599 Kay Seufferheld: Conceptualisation, Data curation, Formal analysis, Investigation, Methodology,
 600 Software, Visualisation, Writing - Original Draft; Pedro V. G. Batista: Conceptualisation, Methodology,
 601 Validation, Writing (review and editing); Hadi Shokati: Writing (review and editing); Thomas Scholten:
 602 Supervision, Writing - Review & Editing; Peter Fiener: Conceptualisation, Data curation, Project
 603 administration, Supervision, Validation, Writing (review and editing).



604 **Competing interests**

605 Pedro V. G. Batista and Peter Fiener serve as Topic Editor and Executive Editor of SOIL, respectively.

606 **Acknowledgments**

607 We acknowledge the valuable dataset from the Forschungsverbund Agrarökosysteme München (FAM). The
 608 scientific activities of the FAM research network were financially supported by the German Federal Ministry of
 609 Education and Research (BMBF 0339370). We thank all researchers and technical staff involved in collecting and
 610 maintaining these long-term datasets, which made this study possible.

611 During the preparation of this work, the authors used Anthropic Claude 3.7 Sonnet to improve the readability
 612 and language of the manuscript. After using this tool, the authors reviewed and edited the content as needed
 613 and take full responsibility for the content of the published article.

614 **Financial support**

615 This research was funded by the German Research Foundation (DFG) through the DYLAMUST project (Project
 616 number: 509809226).

617 **References**

- 618 Aghabeygi, M., Strauss, V., Paul, C., and Helming, K.: Barriers of adopting sustainable soil management
 619 practices for organic and conventional farming systems, *Discover Soil*, 1, 1-11, 10.1007/s44378-024-
 620 00008-1, 2024.
- 621 Alatorre, L. C., Beguería, S., and García-Ruiz, J. M.: Regional scale modeling of hillslope sediment
 622 delivery: A case study in the Barasona Reservoir watershed (Spain) using WATEM/SEDEM, *J HYDROL*,
 623 391, 109-123, 10.1016/j.jhydrol.2010.07.010, 2010.
- 624 Andersson, J. A. and D'Souza, S.: From adoption claims to understanding farmers and contexts: A
 625 literature review of Conservation Agriculture (CA) adoption among smallholder farmers in southern
 626 Africa, *AGR ECOSYST ENVIRON*, 187, 116-132, 10.1016/j.agee.2013.08.008, 2014.
- 627 Auerswald, K. and Fiener, P.: Soil organic carbon storage following conversion from cropland to
 628 grassland on sites differing in soil drainage and erosion history, *SCI TOTAL ENVIRON*, 661, 481-491,
 629 10.1016/j.scitotenv.2019.01.200, 2019.
- 630 Auerswald, K. and Fiener, P.: Assessing the impact of climate change on soil erosion by water, in:
 631 Understanding and preventing soil erosion, Burleigh Dodds Science Publishing Limited, London, 51-76,
 632 10.19103/AS.2023.0131.05, 2024.
- 633 Auerswald, K., Fiener, P., and Dikau, R.: Rates of sheet and rill erosion in Germany — A meta-analysis,
 634 *GEOMORPHOLOGY*, 111, 182-193, 10.1016/j.geomorph.2009.04.018, 2009.
- 635 Auerswald, K., Wilken, F., and Fiener, P.: Soil properties at the Scheyern experimental farm covering 14
 636 small adjacent watersheds and their surroundings [dataset], 10.13140/RG.2.2.14231.83365, 2019a.
- 637 Auerswald, K., Fiener, P., Gerl, G., and Wilken, F.: Land use and land management data from the
 638 Scheyern experimental farm covering 14 small adjacent watersheds and their surroundings [dataset],
 639 10.13140/RG.2.2.26172.49285, 2019b.
- 640 Auerswald, K., Fiener, P., Martin, W., and Elhaus, D.: Use and misuse of the K factor equation in soil
 641 erosion modeling: An alternative equation for determining USLE nomograph soil erodibility values,
 642 *CATENA*, 118, 220-225, 10.1016/j.catena.2014.01.008, 2014.



- 643 Auerswald, K., Kainz, M., Scheinost, A., and Sinowski, W.: The Scheyern Experimental Farm: Research
644 methods, the farming system and definition of the framework of site properties and characteristics, in,
645 183-194, 10.1007/978-3-662-04504-6_10, 2001.
- 646 Batista, P. V. G., Davies, J., Silva, M. L. N., and Quinton, J. N.: On the evaluation of soil erosion models:
647 Are we doing enough?, EARTH-SCI REV, 197, 102898, 10.1016/j.earscirev.2019.102898, 2019.
- 648 Batista, P. V. G., Fiener, P., Scheper, S., and Alewell, C.: A conceptual-model-based sediment connectivity
649 assessment for patchy agricultural catchments, HYDROL EARTH SYST SC, 26, 3753-3770, 10.5194/hess-
650 26-3753-2022, 2022.
- 651 Beven, K.: A manifesto for the equifinality thesis, J HYDROL, 320, 18-36, 10.1016/j.jhydrol.2005.07.007,
652 2006.
- 653 Beven, K.: Towards a methodology for testing models as hypotheses in the inexact sciences, P ROY SOC
654 A-MATH PHY, 475, 20180862, 10.1098/rspa.2018.0862, 2019.
- 655 Beven, K. and Binley, A.: The future of distributed models: Model calibration and uncertainty prediction,
656 HYDROL PROCESS, 6, 279-298, 10.1002/hyp.3360060305, 1992.
- 657 Beven, K. and Lane, S.: On (in)validating environmental models. 1. Principles for formulating a Turing-
658 like Test for determining when a model is fit-for purpose, HYDROL PROCESS, 36, e14704,
659 10.1002/hyp.14704, 2022.
- 660 Brazier, R. E., Beven, K. J., Freer, J., and Rowan, J. S.: Equifinality and uncertainty in physically based soil
661 erosion models: application of the GLUE methodology to WEPP-the Water Erosion Prediction Project-
662 for sites in the UK and USA, EARTH SURF PROCESSES, 25, 825-845, 10.1002/1096-
663 9837(200008)25:8<825::AID-ESP101>3.0.CO;2-3, 2000.
- 664 Brus, D. J. and van den Akker, J. J. H.: How serious a problem is subsoil compaction in the Netherlands?
665 A survey based on probability sampling, SOIL, 4, 37-45, 10.5194/soil-4-37-2018, 2018.
- 666 Carter, C. E. and Parsons, D. A.: Field tests on the coshocton-type wheel runoff sampler, T ASAE, 10,
667 133-135, 10.13031/2013.39613, 1967.
- 668 Choudhury, B. U., Nengzouzam, G., and Islam, A.: Runoff and soil erosion in the integrated farming
669 systems based on micro-watersheds under projected climate change scenarios and adaptation
670 strategies in the eastern Himalayan mountain ecosystem (India), J ENVIRON MANAGE, 309, 114667,
671 10.1016/j.jenvman.2022.114667, 2022.
- 672 Dermisis, D., Abaci, O., Papanicolaou, A. N., and Wilson, C. G.: Evaluating grassed waterway efficiency
673 in southeastern Iowa using WEPP, SOIL USE MANAGE, 26, 183-192, 10.1111/j.1475-
674 2743.2010.00257.x, 2010.
- 675 Desmet, P. J. J. and Govers, G.: A GIS procedure for automatically calculating the USLE LS factor on
676 topographically complex landscape units, J SOIL WATER CONSERV, 51, 427-433,
677 10.1016/j.cageo.2012.09.027, 1996.
- 678 DIN-Normenausschuss, W.: Soil quality - Predicting soil erosion by water by means of ABAG,
679 10.31030/3365455, 2022.
- 680 Dymond, J. R., Betts, H. D., and Schierlitz, C. S.: An erosion model for evaluating regional land-use
681 scenarios, ENVIRON MODELL SOFTW, 25, 289-298, 10.1016/j.envsoft.2009.09.011, 2010.
- 682 Eekhout, J. P. C., Terink, W., and De Vente, J.: Assessing the large-scale impacts of environmental change
683 using a coupled hydrology and soil erosion model, EARTH SURF DYNAM, 6, 687-703, 10.5194/esurf-6-
684 687-2018, 2018.
- 685 Fiener, P. and Auerswald, K.: Effectiveness of grassed waterways in reducing runoff and sediment
686 delivery from agricultural watersheds, J ENVIRON QUAL, 32, 927-936, 10.2134/jeq2003.9270, 2003.
- 687 Fiener, P. and Auerswald, K.: Measurement and modeling of concentrated runoff in grassed waterways,
688 J HYDROL, 301, 198-215, 10.1016/j.jhydrol.2004.06.030, 2005.
- 689 Fiener, P. and Auerswald, K.: Rotation effects of potato, maize, and winter wheat on soil erosion by
690 water, SOIL SCI SOC AM J, 71, 1919-1925, 10.2136/sssaj2006.0355, 2007.
- 691 Fiener, P. and Auerswald, K.: Grassed waterways, in, American Society of Agronomy, Crop Science
692 Society of America, Soil Science Society of America, 131-150, 10.2134/agronmonogr59.c7, 2018.



- 693 Fiener, P., Auerswald, K., and Weigand, S.: Managing erosion and water quality in agricultural
694 watersheds by small detention ponds, *AGR ECOSYST ENVIRON*, 110, 132-142,
695 10.1016/j.agee.2005.03.012, 2005.
- 696 Fiener, P., Wilken, F., and Auerswald, K.: Filling the gap between plot and landscape scale – eight years
697 of soil erosion monitoring in 14 adjacent watersheds under soil conservation at Scheyern, Southern
698 Germany, *Advances in Geosciences*, 48, 31-48, 10.5194/adgeo-48-31-2019, 2019a.
- 699 Fiener, P., Wilken, F., and Auerswald, K.: Runoff and sediment delivery data at the Scheyern
700 experimental farm covering 14 small adjacent watersheds [dataset], 10.13140/RG.2.2.30786.22729,
701 2019b.
- 702 Gonzalez-Hidalgo, J. C., Batalla, R. J., Cerda, A., and de Luis, M.: A regional analysis of the effects of
703 largest events on soil erosion, *CATENA*, 95, 85-90, 10.1016/j.catena.2012.03.006, 2012.
- 704 Gumiere, S. J., Le Bissonnais, Y., Raclot, D., and Cheviron, B.: Vegetated filter effects on sedimentological
705 connectivity of agricultural catchments in erosion modelling: a review, *EARTH SURF PROCESSES*, 36, 3-
706 19, 10.1002/esp.2042, 2011.
- 707 Hessel, R. and Tenge, A.: A pragmatic approach to modelling soil and water conservation measures with
708 a catchment scale erosion model, *CATENA*, 74, 10.1016/j.catena.2008.03.018, 2008.
- 709 Hlavčová, K., Kohnová, S., Velísková, Y., Studvová, Z., Sočuvka, V., and Ivan, P.: Comparison of two
710 concepts for assessment of sediment transport in small agricultural catchments, *J HYDROL*
711 *HYDROMECH*, 66, 404-415, 10.2478/johh-2018-0032, 2018.
- 712 Hosseinzadehtalaei, P., Tabari, H., and Willems, P.: Climate change impact on short-duration extreme
713 precipitation and intensity–duration–frequency curves over Europe, *J HYDROL*, 590, 125249,
714 10.1016/j.jhydrol.2020.125249, 2020.
- 715 Keller, T., Sandin, M., Colombi, T., Horn, R., and Or, D.: Historical increase in agricultural machinery
716 weights enhanced soil stress levels and adversely affected soil functioning, *Soil and Tillage Research*,
717 194, 104293, 10.1016/j.still.2019.104293, 2019.
- 718 Kinnell, P. I. A.: Runoff dependent erosivity and slope length factors suitable for modelling annual
719 erosion using the Universal Soil Loss Equation, *HYDROL PROCESS*, 21, 2681-2689, 10.1002/hyp.6493,
720 2007.
- 721 Montanarella, L., Pennock, D. J., McKenzie, N., Badraoui, M., Chude, V., Baptista, I., Mamo, T., Yemefack,
722 M., Singh Aulakh, M., and Yagi, K.: World's soils are under threat, *SOIL*, 2, 79-82, 10.5194/soil-2-79-
723 2016, 2016.
- 724 Myhre, G., Alterskjær, K., Stjern, C. W., Hodnebrog, Ø., Marelle, L., Samset, B. H., Sillmann, J., Schaller,
725 N., Fischer, E., Schulz, M., and Stohl, A.: Frequency of extreme precipitation increases extensively with
726 event rareness under global warming, *SCI REP-UK*, 9, 16063, 10.1038/s41598-019-52277-4, 2019.
- 727 NAW, D.-N. W.: Soil quality - Predicting soil erosion by water by means of ABAG,
728 <https://dx.doi.org/10.31030/3365455>, 2022.
- 729 Nearing, M.: Why soil erosion models over-predict small soil losses and under-predict large soil losses,
730 *CATENA*, 32, 15-22, 10.1016/S0341-8162(97)00052-0, 1998.
- 731 Nearing, M. A.: Evaluating soil erosion models using measured plot data: accounting for variability in
732 the data, *EARTH SURF PROCESSES*, 25, 1035-1043, 10.1002/1096-9837(200008)25:9<1035::AID-
733 ESP121>3.0.CO;2-B, 2000.
- 734 Nearing, M. A.: Soil erosion and conservation, in: *Environmental Modelling*, edited by: J., W., and M.,
735 M., 365-378, 10.1002/9781118351475.ch22, 2013.
- 736 Notebaert, B., Vaes, B., Verstraeten, G., and Govers, G.: *WaTEM / SEDEM version 2006 Manual*,
737 Onnen, N., Heckrath, G., Stevens, A., Olsen, P., Greve, M. B., Pullens, J. W. M., Kronvang, B., and Van
738 Oost, K.: Distributed water erosion modelling at fine spatial resolution across Denmark,
739 *GEOMORPHOLOGY*, 342, 150-162, 10.1016/j.geomorph.2019.06.011, 2019.
- 740 Peeters, I., Van Oost, K., Govers, G., Verstraeten, G., Rommens, T., and Poesen, J.: The compatibility of
741 erosion data at different temporal scales, *EARTH PLANET SC LETT*, 265, 138-152,
742 10.1016/j.epsl.2007.09.040, 2008.



- 743 Quinn, P., Beven, K., Chevallier, P., and Planchon, O.: The prediction of hillslope flow paths for
 744 distributed hydrological modelling using digital terrain models, *HYDROL PROCESS*, 5, 59-79,
 745 10.1002/hyp.3360050106, 1991.
- 746 Quinton, J. N. and Fiener, P.: Soil erosion on arable land: An unresolved global environmental threat,
 747 *Progress in Physical Geography: Earth and Environment*, 48, 136-161, 10.1177/03091333231216595,
 748 2024.
- 749 Rehm, R. and Fiener, P.: Model-based analysis of erosion-induced microplastic delivery from arable land
 750 to the stream network of a mesoscale catchment, *SOIL*, 10, 211–230, 10.5194/soil-10-211-2024, 2024.
- 751 Renard, K. G.: Predicting soil erosion by water: A guide to conservation planning with the Revised
 752 Universal Soil Loss Equation (RUSLE), *Agricultural handbook*, US Department of Agriculture, Agricultural
 753 Research Service, United States 1997.
- 754 Rickson, R. J., Deeks, L. K., Graves, A., Harris, J. A. H., Kibblewhite, M. G., and Sakrabani, R.: Input
 755 constraints to food production: the impact of soil degradation, *FOOD SECUR*, 7, 351-364,
 756 10.1007/s12571-015-0437-x, 2015.
- 757 Risse, M., Nearing, M. A., Lafen, J. M., and Nicks, A. D.: Error assessment in the Universal Soil Loss
 758 Equation, *SOIL SCI SOC AM J*, 57, 825-833, 10.2136/sssaj1993.03615995005700030032x, 1993.
- 759 Schad, P., Anjos, L., Llobet, J. B., Deckers, S., Dondeyne, S., Eberhardt, E., Gerasimova, M., Harms, B.,
 760 Kabala, C., Mantel, S., Michéli, E., Monger, C., Claret, R. P., Stahr, K., Huyssteen, C. v., Bunes, V., and
 761 Rau, M., IUSS (Ed.): *World Reference Base for Soil Resources. International soil classification system for*
 762 *naming soils and creating legends for soil maps.*, IUSS Working Group WRB, Vienna, Austria, 236
 763 pp. 2022.
- 764 Schwertmann, U., Vogl, W., and Kainz, M.: *Bodenerosion durch Wasser: Vorhersage des Abtrags und*
 765 *Bewertung von Gegenmassnahmen*, Stuttgart: Ulmer, 64 pp. 1987.
- 766 Smith, H. G., Peñuela, A., Sangster, H., Sellami, H., Boyle, J., Chiverrell, R., Schillereff, D., and Riley, M.:
 767 Simulating a century of soil erosion for agricultural catchment management, *EARTH SURF PROCESSES*,
 768 43, 2089-2105, 10.1002/esp.4375, 2018.
- 769 Steegen, A., Govers, G., Nachtergaele, J., Takken, I., Beuselinck, L., and Poesen, J.: Sediment export by
 770 water from an agricultural catchment in the Loam Belt of central Belgium, *GEOMORPHOLOGY*, 33, 25-
 771 36, 10.1016/S0169-555X(99)00108-7, 2000.
- 772 Van Oost, K., Govers, G., and Desmet, P.: Evaluating the effects of changes in landscape structure on
 773 soil erosion by water and tillage, *LANDSCAPE ECOL*, 15, 577-589, 10.1023/A:1008198215674, 2000.
- 774 Van Rompaey, A. J. J., Verstraeten, G., Van Oost, K., Govers, G., and Poesen, J.: Modelling mean annual
 775 sediment yield using a distributed approach, *EARTH SURF PROCESSES*, 26, 1221-1236,
 776 10.1002/esp.275, 2001.
- 777 Verstraeten, G., Van Oost, K., Van Rompaey, A., Poesen, J., and Govers, G.: Evaluating an integrated
 778 approach to catchment management to reduce soil loss and sediment pollution through modelling,
 779 *SOIL USE MANAGE*, 18, 386-394, 10.1111/j.1475-2743.2002.tb00257.x, 2002.
- 780 Wilken, F., Fiener, P., and Auerswald, K.: Topography at the Scheyern experimental farm covering 14
 781 small adjacent watersheds and their surroundings [dataset], 10.13140/RG.2.2.32044.51845, 2019a.
- 782 Wilken, F., Fiener, P., and Auerswald, K.: Meteorological data at the Scheyern experimental farm
 783 covering 14 small adjacent watersheds and their surroundings [dataset],
 784 10.13140/RG.2.2.34561.10088, 2019b.
- 785 Wilken, F., Ketterer, M., Koszinski, S., Sommer, M., and Fiener, P.: Understanding the role of water and
 786 tillage erosion from 239+240Pu tracer measurements using inverse modelling, *SOIL*, 6, 549-564,
 787 10.5194/soil-6-549-2020, 2020.
- 788 Wischmeier, W. H. and Smith, D. D.: *Predicting rainfall erosion losses: A guide to conservation planning*,
 789 *Agriculture Handbook*, 537, Department of Agriculture, Science and Education Administration, United
 790 States, 65 pp. 1978.